

Latent Simplex Position Model: High Dimensional Multi-view Clustering with Uncertainty Quantification

Leo L. Duan*

December 20, 2024

Abstract: High dimensional data often contain multiple facets, and several clustering patterns (views) can co-exist under different feature subspaces. While multi-view clustering algorithms were proposed, the uncertainty quantification remains difficult — a particular challenge is in the high complexity of estimating the cluster assignment probability under each view, or/and to efficiently share information across views. In this article, we propose an empirical Bayes approach — viewing the similarity matrices generated over subspaces as rough first-stage estimates for co-assignment probabilities, in its Kullback-Leibler neighborhood we obtain a refined low-rank soft cluster graph, formed by the pairwise product of simplex coordinates. Interestingly, each simplex coordinate directly encodes the cluster assignment uncertainty. For multi-view clustering, we equip each similarity matrix with a mixed membership over a small number of latent views, leading to effective dimension reduction. With a high model flexibility, the estimation can be succinctly re-parameterized as a continuous optimization problem, hence enjoys gradient-based computation. Theory establishes the connection of this model to random cluster graph under multiple views. Compared to single-view clustering approaches, substantially more interpretable results are obtained when clustering brains from human traumatic brain injury study, using high-dimensional gene expression data.

KEY WORDS: Co-regularized Clustering, Consensus, PAC-Bayes, Random Cluster Graph, Variable Selection

*Department of Statistics, University of Florida, Gainesville, FL, email: li.duan@ufl.edu

1 Introduction

High dimensional data are becoming increasingly common in areas such as genomics, computer vision, neuroscience, etc. They are characterized by the ambient dimension p substantially larger than the sample size n . When clustering such data, canonical solutions tend to focus on finding one particular partition. For example, one idea is to use variable selection method to identify a small subset of variables with large discriminability, then using them as input for clustering algorithms (Tadesse et al., 2005; Hoff, 2006; Witten and Tibshirani, 2010); another idea is to reduce dimension onto latent linear subspaces, often via Gaussian mixture model with low-rank covariance structure (Ghahramani and Hinton, 1996); recent work extends this to variational autoencoder for nonlinear dimension reduction (Dilokthanakul et al., 2016). These methods have been successful when there is only one clear segmentation in the data. However, as high dimension data often contains multiple facets of the observations, it is more natural to consider more than one partition schemes — that is, different subsets of variables can correspond to distinct group structures. As a result, focusing on one partition scheme — or, ‘single-view’ is often inadequate.

There has been an active literature motivated for ‘multi-view clustering’. To be specific, this article focuses on characterizing the multiplicity of the clustering results, as opposed to some alternatives aiming for one consensus from multiple data sources. In this scope, early work includes combining random projection and spectral clustering to obtain clusters on a random subspace, and repeating this for several times to produce multiple clustered views (Fern and Brodley, 2003); using regularization framework by running clustering algorithm in each subspace, while minimizing the cross-view divergence (Joshi et al., 2016; Kumar et al., 2011).

On the other hand, as clusters tend to overlap, there is often substantial amount of uncertainty in clustering. A primary interest is the randomness of cluster assignment, characterized by the categorical probabilities. In canonical single-view setting, one typically relies on Bayesian framework by assigning a model-based likelihood (Fraley and Raftery, 2002). This requires a parametric assumption on each cluster-conditional distribution, then estimating the posterior of cluster assignment via the EM algorithm or Markov-chain Monte Carlo (MCMC). In the Bayesian multi-view context, Indian Buffet Process was utilized to combine relevant features and Gaussian mixture model to produce clustering afterwards (Guan et al., 2010; Niu et al., 2012). The fully Bayesian framework provides an elegant generative perspective for the multi-view data, however, there are two major challenges: (1)

assigning a cluster-conditional distribution is prone to model misspecification, leading to breakdown of parameter estimation (Hennig et al., 2004) and uncontrolled growth in the number of clusters (Miller and Dunson, 2018); (2) the MCMC computation is known to suffer from a critically slow convergence/mixing as dimension grows, limiting its high dimension application. For the former, it was recently shown that modeling pairwise divergence has much better robustness compared to the original data (Duan and Dunson, 2018); for the latter problems in general, it has become especially appealing to replace sampling with optimization-based approximation for a rapid quantification of posterior distribution (El Moselhy and Marzouk, 2012).

In this article, we are motivated for an empirical Bayes approach that allows for a direct estimation of cluster assignment / co-assignment probabilities, in the presence of several alternative clustering patterns. This is inspired by the resemblance between a similarity matrix and a soft cluster graph, hence the former can be consider as a noisy version of the latter. In community detection literature, one often learn a low rank representation for each data point as the latent position in Euclidean / Stiefel space (Hoff et al., 2002), then cluster the coordinates into communities (Handcock et al., 2007). Instead of going through two modeling stages, this article puts the latent coordinate directly on the probability simplex, describing the probability for cluster assignment and allows direct simplex-based optimization; at the same time, each co-assignment matrix can be considered as a convex combination of only a few latent pure views, leading to borrowing of information across views.

2 Method

Let $y_i \in \mathcal{Y}$ be the source data over $i = 1, \dots, n$. The sample space $\mathcal{Y} = \mathcal{Y}^{(1)} \times \dots \times \mathcal{Y}^{(p)}$ is high-dimensional with large p , where each subspace $\mathcal{Y}^{(v)}$ can itself be one- or multi-dimensional. The goal of multi-view clustering is to infer the multiple clustering patterns, for different combination of subspaces. We assume there are d latent alternative clustering patterns, through a convex combination, one can produce an individual clustering view for each subspace. Therefore, we can simply assume there are p views for the data. We denote the i th data point under the v th view by $y_i^{(v)}$, the associated cluster assignment label by $c_i^{(v)} \in \{1, \dots, g\}$, with g the maximum index of clusters over all views.

2.1 Normalized Similarity Matrix

We first use the normalized similarity matrix as a rough first stage estimate for how likely $y_i^{(v)}$ and $y_j^{(v)}$ are in the same cluster.

To formally define, for the v th view, consider a mapping $s^{(v)} : \mathcal{Y}^{(v)} \times \mathcal{Y}^{(v)} \rightarrow [0, 1]$ as

$$s_{i,j}^{(v)} = \mathcal{K}(d_{i,j}^{(v)}), \quad d_{i,j}^{(v)} = \text{div}(y_i^{(v)}, y_j^{(v)}),$$

where $\text{div} : \mathcal{Y}^{(v)} \times \mathcal{Y}^{(v)} \rightarrow [0, \infty)$ is a symmetric divergence (e.g. $\|y_i^{(v)} - y_j^{(v)}\|_2$), and $\mathcal{K} : [0, \infty) \rightarrow [0, 1]$ a non-increasing function. For notation ease, we will use $S^{(v)}$ for the $n \times n$ matrix $\{s_{i,j}^{(v)}\}_{(i,j)}$; further, we assume $S^{(v)}$ is positive semi-definite.

Obviously, computing similarity matrix is almost instantaneous and much easier than estimating from a generative model for y_i . Empirically, with very little effort in tuning, it provides a surprisingly good sketch for cluster structure — as demonstrated by its popularity in the spectral clustering literature (Filippone et al., 2008);. Recently, it was rigorously established (Duan and Dunson, 2018) that certain kernel, such as Laplace $s_{i,j}^{(v)} \propto \exp(-d_{i,j}^{(v)}/b_v)$, automatically accommodates cluster skewness and heavier-than-Gaussian tails. Hence we use this kernel in this article and choose bandwidth b_v according to the method proposed by Zelnik-Manor and Perona (2005).

2.2 Latent Simplex Position Model

Since each $S^{(v)}$ is a rough estimate, we view it as a noisy matrix that appears in the neighborhood of a low rank alternative.

$$S^{(v)} \in \{M : \text{div}(M, A^{(v)}) < \epsilon\}, \quad A^{(v)} = \sum_{l=1}^d \lambda_l^{(v)} W^{(l)} W^{(l)\text{T}}, \quad (1)$$

where $(\lambda_1^{(v)}, \dots, \lambda_d^{(v)})$ is a vector satisfying $\sum_{l=1}^d \lambda_l^{(v)} = 1$ and $\lambda_l^{(v)} \geq 0$; each $W^{(l)}$ is an $n \times g$ matrix, and we denote its i th row by $W_i^{(l)}$; div is a divergence between two matrices that determines the neighborhood.

The interpretation of (1) is that each $A^{(v)}$ is a mix of d pure views $W^{(l)} W^{(l)\text{T}}$, weighted by a mixed membership vector $(\lambda_1^{(v)}, \dots, \lambda_d^{(v)})$. In each pure view, we force $W_i^{(l)}$ to be on a probability simplex

$$w_{i,k}^{(l)} > 0, \quad \sum_{k=1}^g w_{i,k}^{(l)} = 1. \quad (2)$$

Each $W_i^{(l)}$ is a low-dimensional latent position for data y_i , in the l th pure view. This can be taken as a special case of latent position model, coined by Hoff et al. (2002). We name this as latent simplex position model (LSP), and will provide the clustering interpretation in the next section.

With $d \ll p$, it leads to dimension reduction and information sharing. There are two advantages in adopting mixed membership instead of a simple partitioning of views: (1) partitioning requires a discrete combinatorial search and is prohibitively expensive for large p , while here $\lambda_i^{(v)}$ is continuous and hence enables direct optimization; (2) mixed membership allows each feature to be simultaneously considered in multiple pure views, hence allowing two pure views to take information from a common set of features.

To define a loss function, it remains to specify the divergence between $A^{(v)}$ and $S^{(v)}$. It is easy to see that each element in $A^{(v)} = \{a_{i,j}^{(v)}\}_{(i,j)}$ is between $(0, 1)$, so both $s_{i,j}^{(v)}$ and $a_{i,j}^{(v)}$ can be viewed as the success probability for a Bernoulli event (as illustrated later, ‘successfully’ assigning two data into one cluster), therefore, we choose the Kullback-Leibler (KL) divergence,

$$L(S, A) = \sum_{v=1}^p \sum_{i < j} s_{i,j}^{(v)} \left[\log \frac{s_{i,j}^{(v)}}{a_{i,j}^{(v)}} + (1 - s_{i,j}^{(v)}) \log \frac{1 - s_{i,j}^{(v)}}{1 - a_{i,j}^{(v)}} \right]. \quad (3)$$

To provide more intuition, in this model, we assume a ‘true’ clustering structure $A^{(v)}$ living on a low-dimensional manifold, and observe empirical estimate $S^{(v)}$ in its KL neighborhood. Hence minimizing (3) gives a smoothing of $S^{(v)}$. In fact, smoothing via low rank structure has been routinely used in statistics and machine learning literature. As a classical example, in high-dimensional covariance estimation, the fast empirical estimate sample covariance is sub-optimal due to the noise and often lack of positive definiteness, therefore, one uses a near-low rank structure (e.g. spiked covariance) as smoothing (Donoho et al., 2018). In our case, we will theoretically establish why KL divergence is particularly appealing in multi-view setting.

2.3 Simplex Coordinate and Soft Cluster Graph

We now give a clustering interpretation. Consider the event of co-assigning two data into a same cluster. In a pure view case, we can define a cluster graph $\tilde{z}_{i,j}^{(l)} = 1$ if $c_i^{(l)} = c_j^{(l)}$; $\tilde{z}_{i,j}^{(l)} = 0$ if $c_i^{(l)} \neq c_j^{(l)}$. Therefore,

$$\text{pr}(\tilde{z}_{i,j}^{(l)} = 1) = \sum_{k=1}^g \text{pr}(c_i^{(l)} = k) \text{pr}(c_j^{(l)} = k) = W_i^{(l)\text{T}} W_j^{(l)},$$

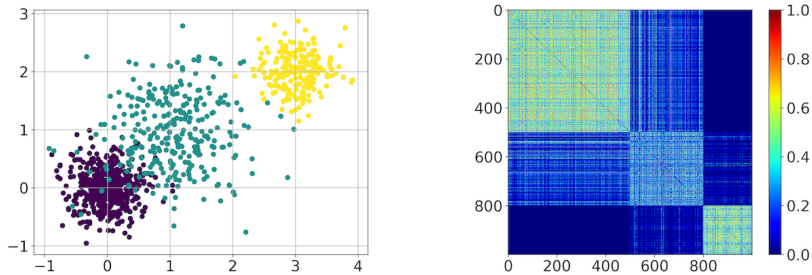
where $w_{i,k}^{(l)} = \text{pr}(c_i^{(l)} = k)$, the assignment probability for assigning $y_i^{(l)}$ to the k th group. We call the graph formed by $\text{pr}(\tilde{z}_{i,j}^{(l)} = 1)$ a soft cluster graph.

In multi-view, we can similarly define a cluster graph $z_{i,j}^{(v)} = 1$, as the result of drawing l th pure view and having $\tilde{z}_{i,j}^{(l)} = 1$; otherwise set $z_{i,j}^{(v)} = 0$. The marginal probability is

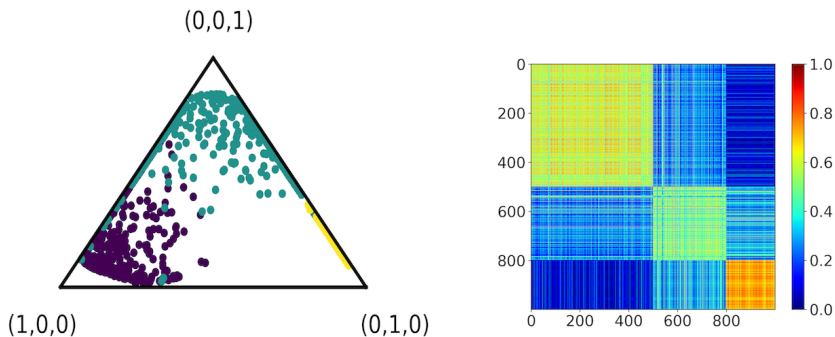
$$\text{pr}(z_{i,j}^{(v)} = 1) = \sum_{l=1}^d \text{pr}(q^{(v)} = l) \text{pr}(\tilde{z}_{i,j}^{(l)} = 1) = \sum_{l=1}^d \lambda_l^{(v)} W_i^{(l)\text{T}} W_j^{(l)},$$

which is exactly the same as (1). We refer to this as the multi-view soft cluster graph. Therefore, the parameter $W_i^{(l)}$ in LSP directly encodes the assignment probabilities for assign y_i to a particular cluster under latent view l .

To illustrate how this represents the uncertainty, we use a simulation. For clear exposition, we focus on a simple case with one view only. The data ($n = 1,000$) are generated from a three-component Gaussian mixture in \mathbb{R}^2 , with the middle cluster having large variance, hence creating large overlap (high uncertainty) [Figure 1(a)]; Figure 1(b) plots the normalized similarity as a noisy but fast estimate for the co-assignment probabilities. Through fitting LSP model, the latent position W_i [Figure 1(c)] provides an estimate for how likely each data can be assigned to a particular cluster (represented by three vertices of the simplex). Figure 1(d) shows the refined co-assignment probability estimate via low-rank smoothing.



(a) The simulated data in \mathbb{R}^2 , the middle cluster (green) has overlap with the other two. (b) Pairwise similarity S matrix as a first stage estimate for co-assignment probability $\text{pr}(c_i = c_j)$.



(c) Simplex coordinates W_i learned from proposed model, representing the clustering uncertainty. Notice the yellow dots are far away from $(1, 0, 0)$, since it has very low probability of getting co-assigned with the violet ones. (d) Soft cluster graph as the refined estimate for co-assignment probability $\text{pr}(c_i = c_j)$ via the low rank estimates $A = WW^T$.

Figure 1: Illustration of how each latent low-rank simplex coordinate provides uncertainty quantification for cluster assignment, and smoothing to produce a soft cluster graph

2.4 Remove Redundant Clusters in Overfitted Model

Often one does not know the minimally needed number of clusters g_0 (or the ‘truth’), and thus needs to assign an overfitted clustering model with $g \gg g_0$. It is useful to reduce the number of effective clusters as much as possible. Equivalently, this is to force all $w_{i,k}^{(l)} = \text{pr}(c_i^{(l)} = k) \approx 0$ for $i = 1, \dots, n$, if

cluster k is redundant.

Since in our model, the assignment probability is now a parameter, hence simple shrinkage can be directly applied on matrix $W^{(l)}$. We use $\ell_{2,1}$ -regularization to induce *column* sparsity in each $W^{(l)}$, leading to regularized loss function

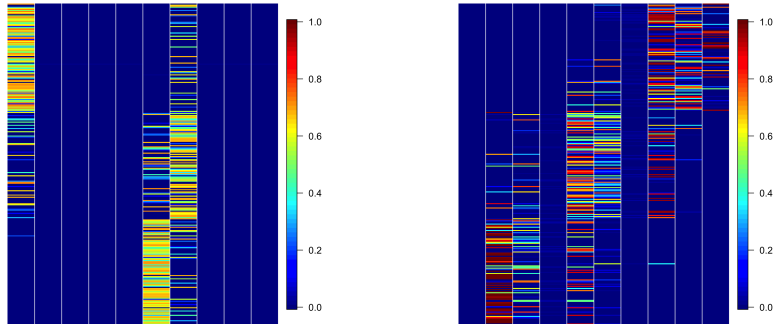
$$L(S, A) + \tau \sum_{l=1}^d \|W^{(l)}\|_{2,1},$$

$$\|W^{(l)}\|_{2,1} = \sum_{k=1}^g \sqrt{\sum_{i=1}^n \{w_{i,k}^{(l)}\}^2}.$$

This regularization is proposed for group lasso variable selection in regression (Yuan and Lin, 2006; Meier et al., 2008), but to our best knowledge, it has not been applied in overfitted clustering model. Figure 2(b) demonstrates its effectiveness in removing redundant clusters.

We also consider classical shrinkage prior on simplex, such as Dirichlet prior with concentration parameter smaller than 1. However, a drawback is that the shrinkage is applied independently on each row, and there is no control on the *joint* distribution of all rows $\{W_i^{(l)}\}_i$. Hence wastefulness can still occur even though each row is sparse. We expect more advanced model such as hierarchical Dirichlet mixture (Teh et al., 2005) (and among others (Zhou, 2014; Ohama et al., 2017)) can solve this problem as well, although we choose $\ell_{2,1}$ penalty for its simplicity.

Remark 1. *In matrix factorization literature, it is more common to consider the nuclear norm (as opposed to the $\ell_{2,1}$ -norm), which is a continuous relaxation for rank regularization (Yan et al., 2017). But for this simplex-based matrix, nuclear norm is in fact ineffective — as a counter-example, consider starting from a certain matrix $W^{(l)}$, one can take a non-zero column, dividing the values equally into 3 column; this adds two wasteful clusters, but does not change the overall matrix rank / nuclear norm.*



(a) Estimated $W^{(l)}$ matrix using $\ell_{2,1}$ regularization. | (b) Estimated $W^{(l)}$ matrix using using row-wise Dirichlet prior $\text{Dir}(0.01, \dots, 0.01)$.

Figure 2: Simulation illustrates the effectiveness of $\ell_{2,1}$ regularization applied on the matrix of simplex coordinates, in an overfitted clustering model with $g = 10$ (with true $g_0 = 3$, panel a).

2.5 Producing Consensus via Combining Different Views

So far we use mixed membership vectors to combine similar views. On the other hand, sometimes it is of interest to combine distinct views to form a ‘consensus’. We now provide an easy solution.

Recall that each view has a mixed membership, $(\lambda_1^{(v)}, \dots, \lambda_d^{(v)})$. We now assign a weight for each view $u_v \geq 0$, such that $\sum_{v=1}^p u_v = 1$.

$$\bar{A} = \sum_{v=1}^p u_v \sum_{l=1}^d \lambda_l^{(v)} W^{(l)} W^{(l)\text{T}} \quad (4)$$

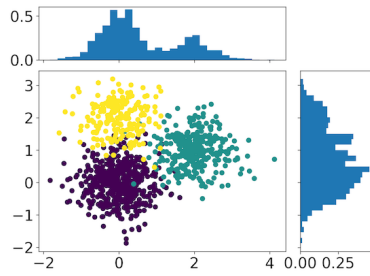
Note that by exchanging summation, this is equivalent to a mixed membership model with membership $(\sum_v u_v \lambda_l^{(v)})$ for pure view l .

The selection of u_v reflects how one defines a consensus. In our case, we choose to exclude the observed views with almost no clustering structure (i.e. for those $A^{(v)}$ close to a rank-1 matrix), and set their $u_v = 0$; then assigning equal weight to each of remaining views — readers may develop other non-equal weight, but we use this for simple exposition.

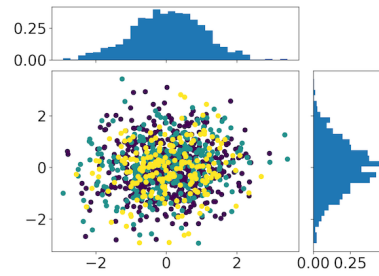
To illustrate, we generate 3 clusters via a Gaussian mixture model in \mathbb{R}^{10} , where the first 2 subspaces having different clustering structures [Figure 3(a)], while the subspace 3 – 10 having no structure [Figure 3(b)]. In the result of fitting in first subspace clustering [Figure 3(c)], the green in (a) is

clearly separated from the other horizontally; while in the result in second subspace (d) is coherent with the fact that the yellow and violet in (a) have very little overlap vertically. Via (4), excluding the noisy subspaces while combining the first two views shows that there are three clear clusters.

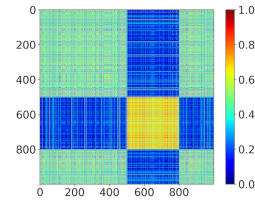
Readers may find some familiarity of this consensus view to the variable selection based clustering. Indeed, the latter can be taken as a special case of having only $d = 2$, with the second view containing no structure. Here, multi-view clustering provides the complete picture.



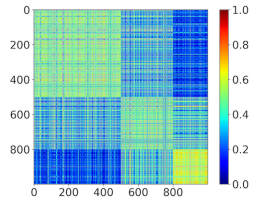
(a) The first two subspaces, each corresponds to different clustering structure.



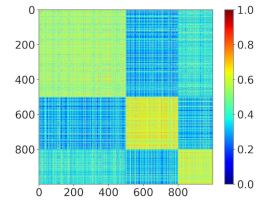
(b) Two noisy subspaces, neither contains any clustering structure.



(c) Estimated $A^{(1)}$ based on the first subspace.



(d) Estimated $A^{(2)}$ based on the second subspace.



(e) Consensus formed by combining the first two subspaces, while ignoring the noisy ones.

Figure 3: Illustration on how one can combine different views in \mathbb{R}^{10} : the first two subspace were taken to produce a consensus, while excluding interfering views with no clustering structure.

3 Theory

In this section, we provide a theoretical justification for the LSP model, on how it is associated with the random cluster graph — the random binary matrix $Z = \{z_{i,j}\}_{(i,j)}$ with $z_{i,j} = 1$ co-assigning two data to the same cluster.

This theory work is an adaptation of Probably Approximately Correct (PAC)-Bayesian bound (Seldin and Tishby, 2010; Germain et al., 2016). To provide some background, consider a random predictor — for each data, one draws a prediction model according to a specified model distribution, makes prediction using the features, and then computes the prediction loss. This loss can be marginalized over the model distribution and the empirical distribution of the data. As the number of data increases, this empirical error would reach the optimal error based on the population.

To extend this idea into multi-view clustering, let us focus on a group of observed views linked to a common pure view. Suppose that we have a common co-assignment probability matrix (which specifies the clustering distribution); one can sample a random cluster graph as a predictor for each observed view. It is then of interest how the clustering error (comparing to the ground truth) changes as the number of views increases.

Similar sampling-based clustering has been done in the Bayesian random partition literature (Blei and Frazier, 2011; Dahl et al., 2017) — using the similarity matrix as the estimated co-assignment probabilities, one sequentially samples cluster assignment for each data point. Intuitively, the performance depends on how good the similarity matrix is as probability estimate; in multi-view, as there are more than one similarities, one could pool similar $S^{(v)}$'s to form improved estimate. With M observed $S^{(v)}$'s associated with a common generating A_0 (which is unobserved); we denote their indices by $v \in V$ and $|V| = M$.

To formalize, let us first describe a way to generate a random cluster graph. Based on $S^{(v)}$ with $v \in V$, one computes a pooled estimate of $n \times n$ co-assignment probability matrix \hat{S} . Then, using this matrix, one can sequentially sample for $i = 2, \dots, n$, $j = 1, \dots, (i - 1)$:

$$\begin{aligned}
 \hat{z}_{i,j} &\sim \text{Bern}(\hat{s}_{i,j}), & \text{if } \forall j' < j, z_{i,j'} = 0, z_{j,j'} = 0, \\
 \hat{z}_{i,j} &= 1, & \text{if } j' < j, z_{i,j'} = 1, z_{j,j'} = 1, \\
 \hat{z}_{i,j} &= 0, & \text{if } j' < j, z_{i,j'} = 0, z_{j,j'} = 1, \\
 \hat{z}_{i,j} &= 0, & \text{if } j' < j, z_{i,j'} = 1, z_{j,j'} = 0,
 \end{aligned} \tag{5}$$

where the second to the forth lines of (5) are due to the deterministic constraints of sequential partition. Slightly abusing notation, let $\hat{Z} \sim \hat{S}$ be the

associated matrix and its drawing distribution.

If the true cluster structure $Z_0^{(v)}$ were known, a loss function can be computed with output in $[0, 1]$ (e.g. such as misclassification rate, 1-minus normalized mutual information, etc.). We denote it by

$$l\left(Z_0^{(v)}, \hat{Z}\right).$$

With M observed views and marginalizing over the random cluster graph distribution (equivalent to sampling \hat{Z} for infinite many times and take average), we have the expected empirical risk,

$$\mathbb{E}_{\hat{Z} \sim \hat{S}} \hat{R}(\hat{Z}) = \frac{1}{M} \sum_{v=1}^M \mathbb{E}_{\hat{Z} \sim \hat{S}} l\left(Z_0^{(v)}, \hat{Z}\right).$$

On the other hand, the optimal would be if we have infinite views, we can compute the population risk

$$\mathbb{E}_{\hat{Z} \sim \hat{S}} R(\hat{Z}) = \mathbb{E}_{Z_0^{(v)} \sim A_0} \mathbb{E}_{\hat{Z} \sim \hat{S}} l\left(Z_0^{(v)}, \hat{Z}\right)$$

It is of interest to see the non-asymptotic rate in M how the empirical approaches the population one, and importantly, what is the leading constant.

Theorem 1. *For $M \in [2, \infty)$, with probability greater than $1 - \delta$ based on A_0 (the generating distribution for $Z_0^{(v)}$), for any specified \hat{S} such that $\hat{Z} \sim \hat{S}$, $\hat{R}(\hat{Z}) \in (0, 1)$, and any smoothing model $A = \{a_{i,j}\}_{(i,j)}$*

$$\begin{aligned} & kl\{\mathbb{E}_{\hat{Z} \sim \hat{S}} \hat{R}(\hat{Z}) \mid \mathbb{E}_{\hat{Z} \sim \hat{S}} R(\hat{Z})\} \\ & \leq \frac{\sum_{j < i} kl(\hat{s}_{i,j} \mid a_{i,j}) + \log\{\exp(\frac{1}{12M}) \sqrt{\frac{\pi M}{2}} + 2\} - \log \delta}{M} \end{aligned}$$

where $kl(a \mid b) = a \log(a/b) + (1-a) \log\{(1-a)/(1-b)\}$ is the Kullbeck-Leibler divergence between two binary distributions.

Therefore, for a given M , it is sensible to minimize the KL divergence in the numerator on the right hand side. Now, it remains to choose a good estimator \hat{S} (so that $\mathbb{E}_{\hat{Z} \sim \hat{S}} R(\hat{Z})$ is reduced toward 0). One intuitive choice

is the sample mean similarity $\hat{S} = (1/M) \sum_{v \in V} S^{(v)}$, yielding

$$\begin{aligned}
& \sum_{j < i} kl\left(\sum_{v \in V} s_{i,j}^{(v)} / M \middle| a_{i,j}\right) \\
&= \frac{1}{M} \sum_{j < i} \sum_{v \in V} \left\{ s_{i,j}^{(v)} \log \frac{\sum_v s_{i,j}^{(v)} / M}{s_{i,j}} + (1 - s_{i,j}^{(v)}) \log \frac{1 - \sum_v s_{i,j}^{(v)} / M}{1 - s_{i,j}} \right\} \\
&+ \frac{1}{M} \sum_{j < i} \sum_{v \in V} \left\{ s_{i,j}^{(v)} \log \frac{a_{i,j}^{(v)}}{a_{i,j}} + (1 - a_{i,j}^{(v)}) \log \frac{1 - a_{i,j}^{(v)}}{1 - a_{i,j}} \right\} \\
&+ \frac{1}{M} \sum_{j < i} \sum_{v \in V} \left\{ s_{i,j}^{(v)} \log \frac{s_{i,j}^{(v)}}{a_{i,j}^{(v)}} + (1 - s_{i,j}^{(v)}) \log \frac{1 - s_{i,j}^{(v)}}{1 - a_{i,j}^{(v)}} \right\}.
\end{aligned}$$

The first part is a constant; the second part is the error due to the mixed membership instead of complete assignment, which is negligible if we choose those v with membership close to one-hot representation. Now, notice the last part is exactly proportional to the loss function $L(S, A)$ for $v \in V$. Therefore, optimizing the LSP loss function effectively minimizes the upper bound of the finite sample error. To put it in a simple way, LSP can be considered as an empirical Bayes estimator for the infinite average model of random cluster graphs.

4 Computation

Since every parameter is continuous, we take advantage of the automatic differentiation toolbox in Tensorflow (Abadi et al., 2015) and momentum-based gradient descent optimizer Adam optimizer (Kingma and Ba, 2014). For simplex vector (w_1, \dots, w_d) , we use softmax representation $w_k = \exp(w_k^*) / \{\sum_{k=1}^d \exp(w_k^*)\}$, where w_k^* is now on the whole real line.

When p is large, it is important to have good initial value to speed up the computation. We notice that when $p \gg n$, the linear space of \mathbb{R}^n is saturated. This means many views will have similar mixed membership. Therefore, we first run a simple K-means algorithm on the columns of y , with $K = d$ (the number of latent views); based on the initial grouping of the columns, we set all the membership vectors in the k th group to be close to one-hot encoding.

Thanks to optimization efficiency, each fitting takes less than 5 minutes, which allows us to tune the parameters easily. For selecting d , we start with a relatively large d and let the model converge to a much smaller value; if

not, we increase the initial d . For choosing τ , we found $\tau = 100$ yields good empirical performance in shrinking simplex.

To produce a point estimate for discrete cluster assignment in each view, it is tempting to simply assign the data to the closest vertex according to $W_i^{(l)}$. However, as shown by Wade et al. (2018), this point-wise optimal often leads substantially sub-optimal clustering. Instead, we again use the estimated $A^{(v)}$ (or consensus \bar{A}) as input in spectral clustering to produce a point estimate; as shown later in the multi-view experiment, using the same algorithm (to produce point estimate), the one based on $A^{(v)}$ is much more accurate than the one based on $S^{(v)}$ (corresponding to the ordinary spectral clustering). This is likely because $A^{(v)}$ is a refined and improved estimate than $S^{(v)}$.

5 Data Experiments

5.1 Single View Experiments

Since most focuses on single view clustering, we first focus on the accuracy of uncertainty quantification and point estimates.

For clear visualization, we start with data from two component mixture distribution, with different degrees of overlap. Figure 4(a-c) plots the results of clustering two Gaussian point clouds under different component variance — as the overlap increases, the assignment probability changes towards the 0.5, as shown in Figure 4(f-h). To compare with the ground truth, we compute the co-assignment probability using Gaussian mixture model. The median absolute deviations (MAD) in the co-assignment probabilities are 0.03, 0.07 and 0.08 in the three cases.

We next deviate from common Gaussian assumption by considering skewed and heavy tails Figure 4(d,e). LSP correctly estimates the uncertainty Figure 4(i,j), with MAD error in co-assignment probabilities 0.07 and 0.06. For point estimates, the misclassification error rates using LSP are 11% and 24%; the ones using spectral clustering (with the same Laplace kernel) are almost identical; as a comparison, the ones using K-means are 26% and 40%.

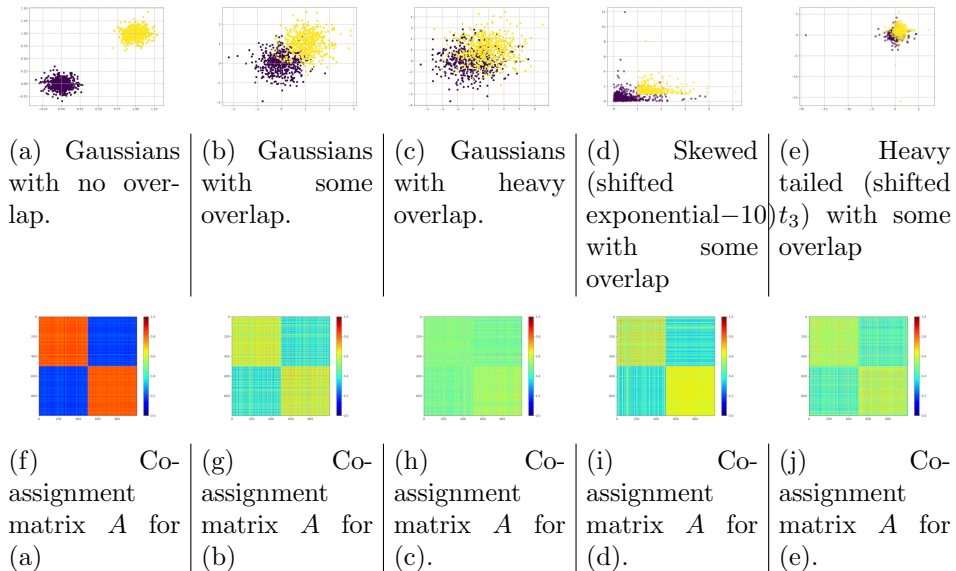


Figure 4: Illustration on uncertainty quantification with different degree of overlap from two point clouds.

5.2 Multi View Experiments

5.2.1 Clustering UCI Hand Written Digits

For comparison with available multi-view clustering method, we consider the UCI hand written digits data previously tested by co-regularized spectral clustering (C-SC) (Kumar et al., 2011). We choose this particular dataset because it does not require specific data processing hence can provide a fair benchmark. The digits data has 6 extracted views: (1) 76 Fourier coefficients of the character shapes, (2) 216 profile correlations, (3) 64 Karhunen-Love coefficients, (4) 240 pixel averages in 2×3 windows, (5) Zernike moments and (6) 6 morphological features. For each view, we use the Laplace kernel for computing the similarity. For each digit, there are 200 samples; the normalized mutual information (NMI) is calculated as a evaluating criterion.

We start with $d = 6$ latent views and the mixed membership converges to effectively only 2 latent classes. When combining views to produce a consensus, LSP has performance almost indistinguishable from C-SC (Table 1). Besides point estimate, the unique advantage of LSP is provides uncertainty quantification for each view. As shown in Figure 5, in the first pure view, the main source of clustering error is largely due to the overlap between first

and the ninth clusters; whereas the second pure view has larger overlaps among clusters.

Combining Multi View						
SV-SC (feature concat)	0.619					
C-SC	0.768					
LSP	0.742					
Single View	1	2	3	4	5	6
SV-SC using Similarity	0.571	0.618	0.646	0.635	0.523	0.474
C-SC best view	0.641	-	-	-	-	-
LSP	0.697	0.706	0.697	0.705	0.705	0.474

Table 1: Normalized mutual information for clustering UCI hand-written digits on each view.

For each observed view, the mixed membership shows that view 1–5 is very close to the first latent view, while view 6 is close to the second latent one. To see if the probability matrix $A^{(v)}$ is a better estimate than the raw $S^{(v)}$, we obtain point estimate in each view using $A^{(v)}$, and compare the result against single view spectral clustering (SV-SC) on each $S^{(v)}$. In the result, LSP produces clearly higher NMI in almost every view (except view 6).

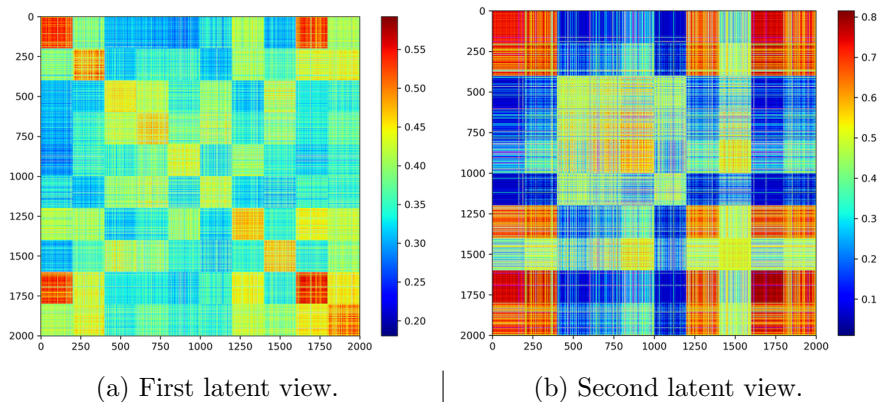


Figure 5: Uncertainty for clustering hand written digit data, represented in the two latent views.

5.2.2 Clustering Brains via RNA-Sequencing Data

We now consider a scientific application with the RNA Sequencing data originated from the human aging, dementia and traumatic brain injury (TBI) study. The data are obtained from Allen Institute for Brain Science (Miller et al., 2017), and the hippocampus region is chosen for its important role in aging-related disease. There are $n = 94$ brains. The age of the subjects at death has the average 90 and standard deviation 6. There are 50,281 genes, each with expression recorded as greater than or equal to zero. Since most of the genes contain very little discriminability, a screening step is first carried out to accelerate the computation: the genes are ranked by their standard deviation divided by the median, with the top $p = 1,000$ chosen for the downstream modeling.

This experiment clusters the 94 brains using the gene expression. The LSP model was initialized at $d = 30$ and $g = 30$. The model quickly converges to effectively 10 different latent views and at most 4 non-trivial clusters.

For validation, the multi-view results are compared against 11 other clinical covariates — such as sex, whether had TBI, dementia evaluation scores, etc. Then the NMI is computed by comparing point estimates from each gene against each clinical covariates (in order to compute NMI for those continuous covariates, they are discretized using median thresholding).

To check if there is a link between some gene(s) and each clinical covariate, the maximum NMI is taken over all genes and reported in Figure 6(a). To provide a reference baseline, a randomly generated Bernoulli distribution with probability 0.1 – 0.9 can produce NMI at most 10% to each covariate; alternatively, the covariate sex (maximum NMI 13%) can be used as a control variable, as it is discovered no obvious effect on the hippocampus area in an early meta-analysis study (Tan et al., 2016). To show that there is strong signal, 20% is shown as the cut-off in the plot. Clearly, there are genes showing a strong link to the clinical covariate.

Among all covariates, the CERAD score (measuring the progression of Alzheimer’s disease), Braak stage (measuring the progression of Parkinson’s disease and Alzheimer’s disease) and confirmed diagnose of Alzheimer disease are strongly linked to a subset of gene expression. For the covariates seemingly less relevant to gene expression, the length of education also shows strong NMI, while the experience of traumatic brain injury (TBI), aging and dementia-related score show surprisingly low or almost no similarity to the gene expression.

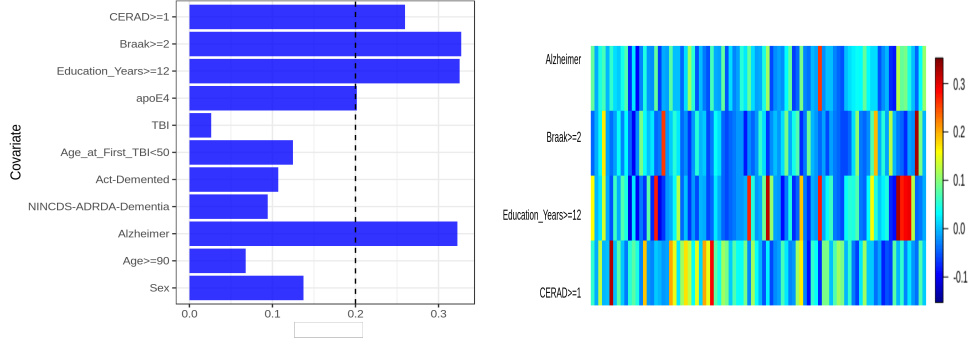
Besides the maximum NMI, Figure 6(b) plots the NMIs of the top 100

genes associated with the selected four covariates. Clearly, each covariate is linked to a unique set of genes, corresponding to a distinct subspace. This unique-subspace finding suggests there would be dire consequences for single-view clustering: for a single-view clustering using all genes, it would suffer from a ‘cancellation’ of discriminabilities, preventing the finding of meaningful clusters. To corroborate, Pearson correlations of the 1,000 genes are calculated among 94 brains — all the correlations are very high with the minimum 96.8%.

As the last step, we compare the results against: LSP consensus view and ℓ_1 -regularized K-means (Witten and Tibshirani, 2010) as a variable selection clustering (we cannot do co-regularized spectral clustering due to the large number of views). The LSP consensus shows only maximum 11.1% NMI, confirming the cancellation effect exist for this data; on the other hand, ℓ_1 -regularized K-means shows maximum 15% NMI related to dementia.

6 Discussion

In this article, assigning each data point with a latent simplex coordinate dramatically simplifies the task for uncertainty quantification in clustering, allowing easy borrowing of information across high-dimensional space. There are several extensions worth pursuing based on the current work: 1. handling the similarity matrix can be computationally prohibitive when n is large, therefore, a random feature map (Rahimi and Recht, 2008) could be considered for linear scalability; 2. one could consider some domain-specific algorithm for combining views — for example, in image processing, one could use a block convolution of neighboring pixels as one view.



(a) Maximum NMI over all genes, using clustering results produced by multi-view LSP model and comparing against each of 11 clinical covariates. (b) The NMI of 100 selected genes linked to four covariates.

Figure 6: Clustering aging brains using gene expression. The results are compared with 11 clinical covariates using NMI.

A Proof of the Main Theorem

Proof. Let $\text{KL}(S||A)$ be the Kullback-Leibler divergence between two generating distributions for a cluster graph using S or A as the co-assignment probability matrix. The sample space of the distribution is a subset of $\{0, 1\}^{n \times (n-1)/2}$ subject to constraints described in (5).

Step 1. Change of measure:

This step is an adaptation of the classic PAC-Bayesian theorem.

$$\begin{aligned}
 & \mathbb{E}_{\hat{Z} \sim \hat{S}} \text{Mkl}(\hat{R}(\hat{Z}), \mathbb{E}_{\hat{Z} \sim \hat{S}} R(\hat{Z})) \\
 & \leq \mathbb{E}_{\hat{Z} \sim \hat{S}} \text{Mkl}(\hat{R}(\hat{Z}), R(\hat{Z})) \\
 & \leq \text{KL}(\hat{S}||A) + \log \mathbb{E}_{\hat{Z} \sim A} \exp[\text{Mkl}\{\hat{R}(\hat{Z}), R(\hat{Z})\}],
 \end{aligned}$$

where the first inequality uses the convexity of the kl function, the second inequality uses the change of measure inequality [Lemma 4 in (Seldin and Tishby, 2010)].

Note that $\hat{R}(\hat{Z}) = (1/M) \sum_{v=1}^M l(Z_0^{(v)}, \hat{Z})$ is a function of random $Z_0^{(1)}, Z_0^{(2)}, \dots, Z_0^{(M)}$,

with probability greater than $1 - \delta$,

$$\begin{aligned}
& \mathbb{E}_{\hat{Z} \sim A} \exp[Mkl\{\hat{R}(\hat{Z}), R(\hat{Z})\}] \\
& \leq \frac{1}{\delta} \mathbb{E}_{Z^{(1)}, \dots, Z^{(M)} \sim A_0} \mathbb{E}_{\hat{Z} \sim A} \exp[Mkl\{\hat{R}(\hat{Z}), R(\hat{Z})\}] \\
& = \frac{1}{\delta} \mathbb{E}_{\hat{Z} \sim A} \mathbb{E}_{Z^{(1)}, \dots, Z^{(M)} \sim A_0} \exp[Mkl\{\hat{R}(\hat{Z}), R(\hat{Z})\}]
\end{aligned}$$

where the inequality is due to Markov's inequality, and the equality due to Fubini's theorem since $\hat{R}(\hat{Z}) \in (0, 1)$, $kl\{\hat{R}(\hat{Z}), R(\hat{Z})\} < \infty$.

Step 2. Bounding the exponential kl function by a constant:

Note that $\mathbb{E}_{Z_0^{(v)} \sim A_0} l(Z_0^{(v)}, \hat{Z}) = R(\hat{Z})$, using Theorem 1 of (Maurer, 2004),

$$\begin{aligned}
& \mathbb{E}_{Z_0^{(1)}, \dots, Z_0^{(M)} \sim A_0} \exp[Mkl\{\hat{R}(\hat{Z}), R(\hat{Z})\}] \\
& \leq \exp\left(\frac{1}{12M}\right) \sqrt{\frac{\pi M}{2}} + 2.
\end{aligned}$$

Step 3. Relaxing the KL-divergences between two cluster graph distributions to total elementwise kl divergences:

Denote \mathcal{Z} by the constrained space inside $\{0, 1\}^{n(n-1)/2}$.

$$\begin{aligned}
\text{KL}(\hat{S}||A) &= \sum_{Z \in \mathcal{Z}} \{1(z_{i,j} = 1) \hat{s}_{i,j} \log \frac{\hat{s}_{i,j}}{a_{i,j}} \\
& \quad + 1(z_{i,j} = 0) (1 - \hat{s}_{i,j}) \log \frac{1 - \hat{s}_{i,j}}{1 - a_{i,j}}\} \\
& \leq \sum_{Z \in \{0,1\}^{n(n-1)/2}} \{1(z_{i,j} = 1) \hat{s}_{i,j} \log \frac{\hat{s}_{i,j}}{a_{i,j}} \\
& \quad + 1(z_{i,j} = 0) (1 - \hat{s}_{i,j}) \log \frac{1 - \hat{s}_{i,j}}{1 - a_{i,j}}\} \\
& = \sum_{j < i} kl(\hat{s}_{i,j} || a_{i,j}),
\end{aligned}$$

where the inequality is due to the non-negativity of each kl function and $\mathcal{Z} \subseteq \{0, 1\}^{n(n-1)/2}$.

Combining the results yields

$$\begin{aligned}
& kl(\mathbb{E}_{\hat{Z} \sim \hat{S}} \hat{R}(\hat{Z}), \mathbb{E}_{\hat{Z} \sim \hat{S}} R(\hat{Z})) \\
& \leq \frac{\sum_{j < i} kl(\hat{s}_{i,j} || a_{i,j}) + \log\{\exp(\frac{1}{12M}) \sqrt{\frac{\pi M}{2}} + 2\} - \log \delta}{M}
\end{aligned}$$

□

References

- Abadi, M., A. Agarwal, P. Barham, E. Brevdo, Z. Chen, C. Citro, G. S. Corrado, A. Davis, J. Dean, M. Devin, S. Ghemawat, I. Goodfellow, A. Harp, G. Irving, M. Isard, Y. Jia, R. Jozefowicz, L. Kaiser, M. Kudlur, J. Levenberg, D. Mané, R. Monga, S. Moore, D. Murray, C. Olah, M. Schuster, J. Shlens, B. Steiner, I. Sutskever, K. Talwar, P. Tucker, V. Vanhoucke, V. Vasudevan, F. Viégas, O. Vinyals, P. Warden, M. Wattenberg, M. Wicke, Y. Yu, and X. Zheng (2015). TensorFlow: Large-scale machine learning on heterogeneous systems.
- Blei, D. M. and P. I. Frazier (2011). Distance dependent Chinese restaurant processes. *Journal of Machine Learning Research* 12(Aug), 2461–2488.
- Dahl, D. B., R. Day, and J. W. Tsai (2017). Random partition distribution indexed by pairwise information. *Journal of the American Statistical Association* 112(518), 721–732.
- Dilokthanakul, N., P. A. Mediano, M. Garnelo, M. C. Lee, H. Salimbeni, K. Arulkumaran, and M. Shanahan (2016). Deep unsupervised clustering with Gaussian mixture variational autoencoders. *arXiv preprint arXiv:1611.02648*.
- Donoho, D. L., M. Gavish, and I. M. Johnstone (2018). Optimal shrinkage of eigenvalues in the spiked covariance model. *Annals of statistics* 46(4), 1742.
- Duan, L. L. and D. B. Dunson (2018). Bayesian distance clustering. *arXiv preprint arXiv:1810.08537*.
- El Moselhy, T. A. and Y. M. Marzouk (2012). Bayesian inference with optimal maps. *Journal of Computational Physics* 231(23), 7815–7850.
- Fern, X. Z. and C. E. Brodley (2003). Random projection for high dimensional data clustering: A cluster ensemble approach. In *Proceedings of the 20th International Conference On Machine Learning*, pp. 186–193.
- Filippone, M., F. Camastra, F. Masulli, and S. Rovetta (2008). A survey of kernel and spectral methods for clustering. *Pattern recognition* 41(1), 176–190.
- Fraley, C. and A. E. Raftery (2002, June). Model-based clustering, discriminant analysis, and density estimation. *Journal of the American Statistical Association* 97(458), 611–631.

- Germain, P., F. Bach, A. Lacoste, and S. Lacoste-Julien (2016). PAC-Bayesian theory meets Bayesian inference. In *Advances in Neural Information Processing Systems*, pp. 1884–1892.
- Ghahramani, Z. and G. E. Hinton (1996). The EM algorithm for mixtures of factor analyzers. Technical report, Technical Report CRG-TR-96-1, University of Toronto.
- Guan, Y., J. G. Dy, D. Niu, and Z. Ghahramani (2010). Variational inference for nonparametric multiple clustering. In *MultiClust Workshop, KDD-2010*.
- Handcock, M. S., A. E. Raftery, and J. M. Tantrum (2007). Model-based clustering for social networks. *Journal of the Royal Statistical Society: Series A (Statistics in Society)* 170(2), 301–354.
- Hennig, C. et al. (2004). Breakdown points for maximum likelihood estimators of location–scale mixtures. *The Annals of Statistics* 32(4), 1313–1340.
- Hoff, P. D. (2006). Model-based subspace clustering. *Bayesian Analysis* 1(2), 321–344.
- Hoff, P. D., A. E. Raftery, and M. S. Handcock (2002). Latent space approaches to social network analysis. *Journal of the American Statistical Association* 97(460), 1090–1098.
- Joshi, S., J. Ghosh, M. Reid, and O. Koyejo (2016). Rényi divergence minimization based co-regularized multiview clustering. *Machine Learning* 104(2-3), 411–439.
- Kingma, D. P. and J. Ba (2014). Adam: A method for stochastic optimization. *arXiv preprint arXiv:1412.6980*.
- Kumar, A., P. Rai, and H. Daume (2011). Co-regularized multi-view spectral clustering. In *Advances in Neural Information Processing Systems*, pp. 1413–1421.
- Maurer, A. (2004). A note on the PAC Bayesian theorem. *arXiv preprint cs/0411099*.
- Meier, L., S. Van De Geer, and P. Bühlmann (2008). The group lasso for logistic regression. *Journal of the Royal Statistical Society: Series B (Statistical Methodology)* 70(1), 53–71.

- Miller, J. A., A. Guillozet-Bongaarts, L. E. Gibbons, N. Postupna, A. Renz, A. E. Beller, S. M. Sunkin, L. Ng, S. E. Rose, and K. A. Smith (2017). Neuropathological and transcriptomic characteristics of the aged brain. *Elife* 6, e31126.
- Miller, J. W. and D. B. Dunson (2018). Robust Bayesian inference via coarsening. *Journal of the American Statistical Association*, in press.
- Niu, D., J. Dy, and Z. Ghahramani (2012). A nonparametric bayesian model for multiple clustering with overlapping feature views. In *Artificial Intelligence and Statistics*, pp. 814–822.
- Ohama, I., I. Sato, T. Kida, and H. Arimura (2017). On the model shrinkage effect of gamma process edge partition models. In *Advances in Neural Information Processing Systems*, pp. 397–405.
- Rahimi, A. and B. Recht (2008). Random features for large-scale kernel machines. In *Advances in Neural Information Processing Systems*, pp. 1177–1184.
- Seldin, Y. and N. Tishby (2010). PAC-Bayesian analysis of co-clustering and beyond. *Journal of Machine Learning Research* 11(Dec), 3595–3646.
- Tadesse, M. G., N. Sha, and M. Vannucci (2005). Bayesian variable selection in clustering high-dimensional data. *Journal of the American Statistical Association* 100(470), 602–617.
- Tan, A., W. Ma, A. Vira, D. Marwha, and L. Eliot (2016). The human hippocampus is not sexually-dimorphic: meta-analysis of structural mri volumes. *Neuroimage* 124, 350–366.
- Teh, Y. W., M. I. Jordan, M. J. Beal, and D. M. Blei (2005). Sharing clusters among related groups: Hierarchical Dirichlet processes. In *Advances in Neural Information Processing Systems*, pp. 1385–1392.
- Wade, S., Z. Ghahramani, et al. (2018). Bayesian cluster analysis: Point estimation and credible balls (with discussion). *Bayesian Analysis* 13(2), 559–626.
- Witten, D. M. and R. Tibshirani (2010). A framework for feature selection in clustering. *Journal of the American Statistical Association* 105(490), 713–726.

- Yan, B., P. Sarkar, and X. Cheng (2017). Provable estimation of the number of blocks in block models. *arXiv preprint arXiv:1705.08580*.
- Yuan, M. and Y. Lin (2006). Model selection and estimation in regression with grouped variables. *Journal of the Royal Statistical Society: Series B (Statistical Methodology)* 68(1), 49–67.
- Zelnik-Manor, L. and P. Perona (2005). Self-tuning spectral clustering. In *Advances in Neural Information Processing Systems*, pp. 1601–1608.
- Zhou, M. (2014). Beta-negative binomial process and exchangeable random partitions for mixed-membership modeling. In *Advances in Neural Information Processing Systems*, pp. 3455–3463.